JACS
JOURNAL OF THE AMERICAN CHEMICAL SOCIETY
Article
pubs.acs.org/JACS

Helical Foldamers Incorporating Photoswitchable Residues for Light-Mediated Modulation of Conformational Preference

Daniela Mazzier,[†] Marco Crisma,[‡] Matteo De Poli,[§] Giulia Marafon,[†] Cristina Peggion,[†] Jonathan Clayden,*[,∥] and Alessandro Moretto*[,†,‡]

[†]Department of Chemical Sciences, University of Padova, Via Marzolo 1, 35131 Padova, Italy
[‡]Institute of Biomolecular Chemistry, Padova Unit, CNR, Via Marzolo 1, 35131 Padova, Italy
[§]School of Chemistry, University of Manchester, Oxford Road, Manchester M13 9PL, United Kingdom
[∥]School of Chemistry, University of Bristol, Cantock's Close, Bristol BS8 1TS, United Kingdom

Supporting Information

ABSTRACT: An *E* unsaturated fumaramide linkage may be introduced into Aib peptide foldamer structures by standard coupling methods and photoisomerized to its *Z* (maleamide) isomer by irradiation with UV light. As a result of the photoisomerization, a new hydrogen-bonded contact becomes possible between the peptide domains located on either side of the unsaturated linkage. Using the fumaramide/maleamide linker to couple a chiral and an achiral fragment allows the change in hydrogen bond network to communicate a conformational preference, inducing a screw sense preference in the achiral domain of the maleamide-linked foldamers that is absent from the fumaramides. Evidence for the induced screw sense preference is provided by NMR and CD, and also by the turning on by light of the diastereoselectivity of a peptide chain extension reaction. The fumaramide/maleamide linker thus acts as a "conformational photodiode" that conducts stereochemical information as a result of irradiation by UV light.

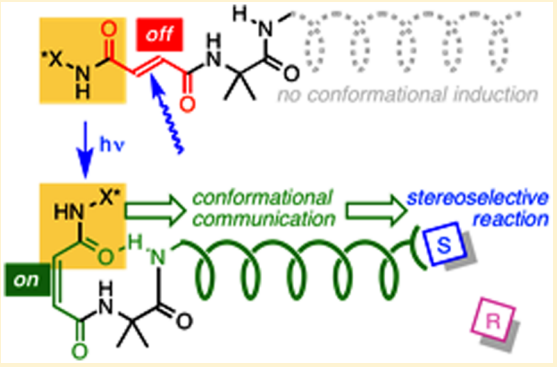

INTRODUCTION

The ability of light to control biochemical mechanisms underpins responses in almost all groups of living organisms: phototaxis in prokaryotes,[1] phototropism in vascular plants and fungi,[2] and vision in animals.[3,4] Sensitivity to light is typically mediated by a protein scaffold hosting a covalently or noncovalently bound chromophore. In vertebrates, vision is mediated by rhodopsin,[5−7] a covalent conjugate formed from a protein, opsin, with a chromophore, retinal. Upon absorption of a photon, the retinal chromophore isomerizes from the 11-*cis* to the all-*trans* configuration. As a result of this localized structural change, a conformational reorganization is induced, which propagates through the tertiary structure of the opsin, allowing it to activate the messenger protein transducin, and ultimately induce hyperpolarization of the photoreceptor cells.[8,9] Artificially modified photoresponsive proteins follow the same pattern, in which a photoswitchable chromophore is conjugated with a protein,[10,11] and the developing field of photopharmacology uses the interaction of photoswitchable, biologically active small molecules with proteins to control a variety of biochemical responses.[12]

Foldamers are synthetic, conformationally defined mimics of proteins and other biopolymers.[13−19] Foldamer structures allow chemists to broaden and diversify the more limited range of structural components that build up natural proteins, and foldamers have been designed to carry out protein-like functions of binding, catalysis and signal relay. Photoswitchable foldamers would allow these functions to be controlled by light.[20] Some of us recently reported a series of synthetic but biomimetic helical foldamers, members of which embed themselves into phospholipid bilayers in a manner reminiscent of rhodopsin, in which global conformational changes result from photoinduced geometrical inversion of an azobenzene chromophore.[21,22]

Azobenzene units have found particularly broad utility as photoswitches, and the replacement of individual monomers of the backbone of an aromatic foldamer by azobenzenes allows gross conformational changes to be induced in the foldamer.[23] A much less commonly exploited chromophore is the *E*/*Z* switchable maleamide/fumaramide unit. This pair of photochemically interconvertible diamides was previously employed in the field of molecular machines as a switchable component of peptide-based [2]rotaxanes.[24,25] It occurred to us that this compact dicarboxamide structure would be particularly suitable for incorporation as a photoswitchable backbone residue in aliphatic, protein-like foldamers, and in this paper we describe the design, synthesis and photoswitchable function of helical

Received: April 29, 2016
Published: June 3, 2016

DOI: 10.1021/jacs.6b04435
J. Am. Chem. Soc. 2016, 138, 8007−8018

Scheme 1. Conversion of Fumaric Acid Derivative 1 to a Series of Fumaramide Peptides 2a–f and Photoisomerization to Their Maleamide Isomers 3a–f

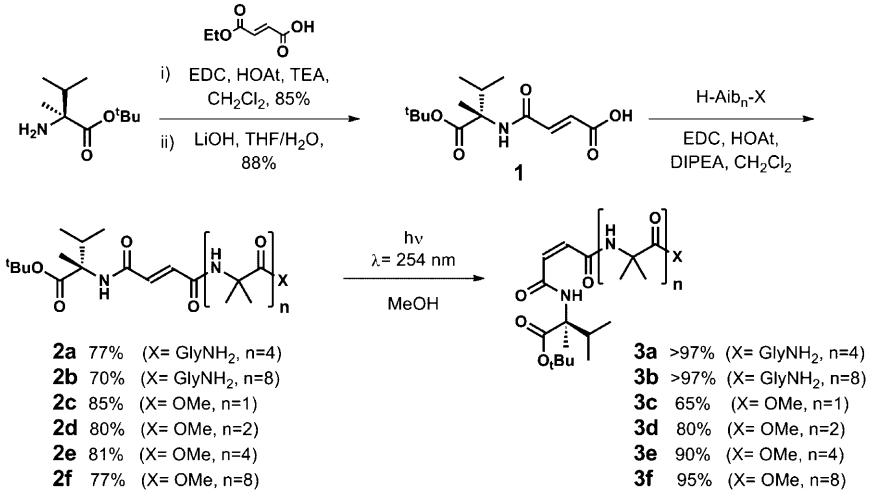

peptidomimetic foldamers containing fumaramide/maleamide residues.

The ability of dynamic foldamers to propagate conformational modifications allows them to behave as communication devices. For example, asymmetric induction can be achieved over lengths of up to 4 nm by exploiting the tendency of a helical chain of achiral quaternary amino acids to adopt the preferred screw sense induced by a terminal chiral residue.[26,28] In the molecules we present here, a *trans* configuration in the fumaramide linkage breaks the hydrogen-bonded chain of conformational induction that underpins such communication mechanisms, while photoisomerization to the *cis* maleamide configuration restores the conformational communication between two helical domains of the peptide.

RESULTS AND DISCUSSION

Conformational Consequences of Photochemical Switching. In order to explore the ability of the fumaramide/maleamide switch to conduct or interrupt conformational communication in response a photochemical switch, a fumaramide residue was introduced by stepwise amide bond formation on one side to the N terminus of a series of oligomers built from the achiral quaternary α-amino acid α-aminoisobutyric acid (Aib), and on the other side to a chiral residue capable of inducing these Aib oligomers to adopt a conformational screw-sense preference (Scheme 1). Examples of screw-sense bias in related achiral Aib-rich oligomers to which a chiral controller is *directly* attached have been reported.[29−33] Oligomers of Aib typically adopt well-defined 3_{10}-helical structures both in solution and in the crystal state,[34,35] but because each individual amino acid possesses a plane of symmetry, in solution the helices exist as a rapidly interconverting[36,37] equal mixture of left- and right-handed screw-sense conformers. The conformational preferences of the chiral residue L-(αMe)Val are closely comparable to those of achiral Aib, in that this quaternary α-amino acid is an effective promoter of folded, helical conformations,[29,38−40] and among the chiral C^{α}-methylated analogues of proteinogenic amino acids, the C^{β}-branched (αMe)Val residue exerts the strongest bias in favor of a single helical screw sense [right-handed for L-(αMe)Val].[41,42] Incorporating this chiral quaternary residue into our model system was expected to maximize the chances of communication of chiral information across the unsaturated diamide linkage.

Monoethyl fumarate was coupled with H-L-(αMe)Val-O*t*Bu under standard coupling conditions (EDC/HOAt) to give the carboxylic acid **1** after basic hydrolysis (Scheme 1). Functionalized Aib oligomers **2a–f** were obtained by reaction of activated **1** (EDC/HOAt) with Aib homopeptides H-Aib$_n$-X. The first pair of compounds (**2a,b**) contains a C-terminal glycinamide residue to provide a ^{1}H NMR reporter of screw-sense preference,[42,43] while a second group of compounds, namely **2c–f** (Scheme 1), provides a series of Aib homopeptide methyl esters of increasing length (1, 2, 4, or 8 Aib residues). The six fumaramide peptides **2a–f** were isomerized to their corresponding maleamide (*Z*) isomers **3a–f** in 65–97% selectivity (determined by NMR) by irradiation (UV light at 254 nm) of solutions in MeOH. As photoisomerization with UV light gave only 65% conversion of **2c** (*E*) to **3c** (*Z*) (SI, Figure S7), **3c** was synthesized directly from maleic anhydride (see SI). For all of the other compounds listed in Scheme 1, photoisomerization allowed conversion to the *Z* isomers with selectivity ≥80%. In particular, the isomerization of **2a** to **3a** was almost quantitative in 1 h, and pure sample maleamide **3a** was obtained by HPLC.

The consequences of the isomerization of the *E* double bond of **2a** to the *Z* double bond of **3a** were initially investigated using 2D-NMR (NOESY) experiments in CD_3CN (see Supporting Information). A series of sequential αNH(i)→ αNH(i + 1) and βCH$_3$(i) → αNH(i + 1), and other medium range βCH$_3$(i)→ αNH(i + 2) connectivities, characteristic of a well-developed helical conformation,[44] were evident in the NOESY spectra of both **2a** and **3a** (SI, Figures S1–S3). These findings suggest that the -(Aib)$_4$- segment is indeed folded into a helical conformation, as expected, and that the helix remains unchanged by the isomerization process.

In a 3_{10}-helix formed by an N-acylated peptide, the NH groups of the first and second residues do not participate in the intramolecular H-bonding network. Comparison of the 1D ^{1}H NMR spectra of peptides **2a** and **3a** (Figure 1A) reveals significantly different chemical shifts for the NH signals of Aib(2) and L-(αMe)Val in the two isomers. In particular, the Aib(2) NH signal moves sharply downfield upon isomerization from **2a** to the *Z* isomer **3a** (from 7.14 to 8.61 ppm). This

DOI: 10.1021/jacs.6b04435
J. Am. Chem. Soc. 2016, 138, 8007−8018

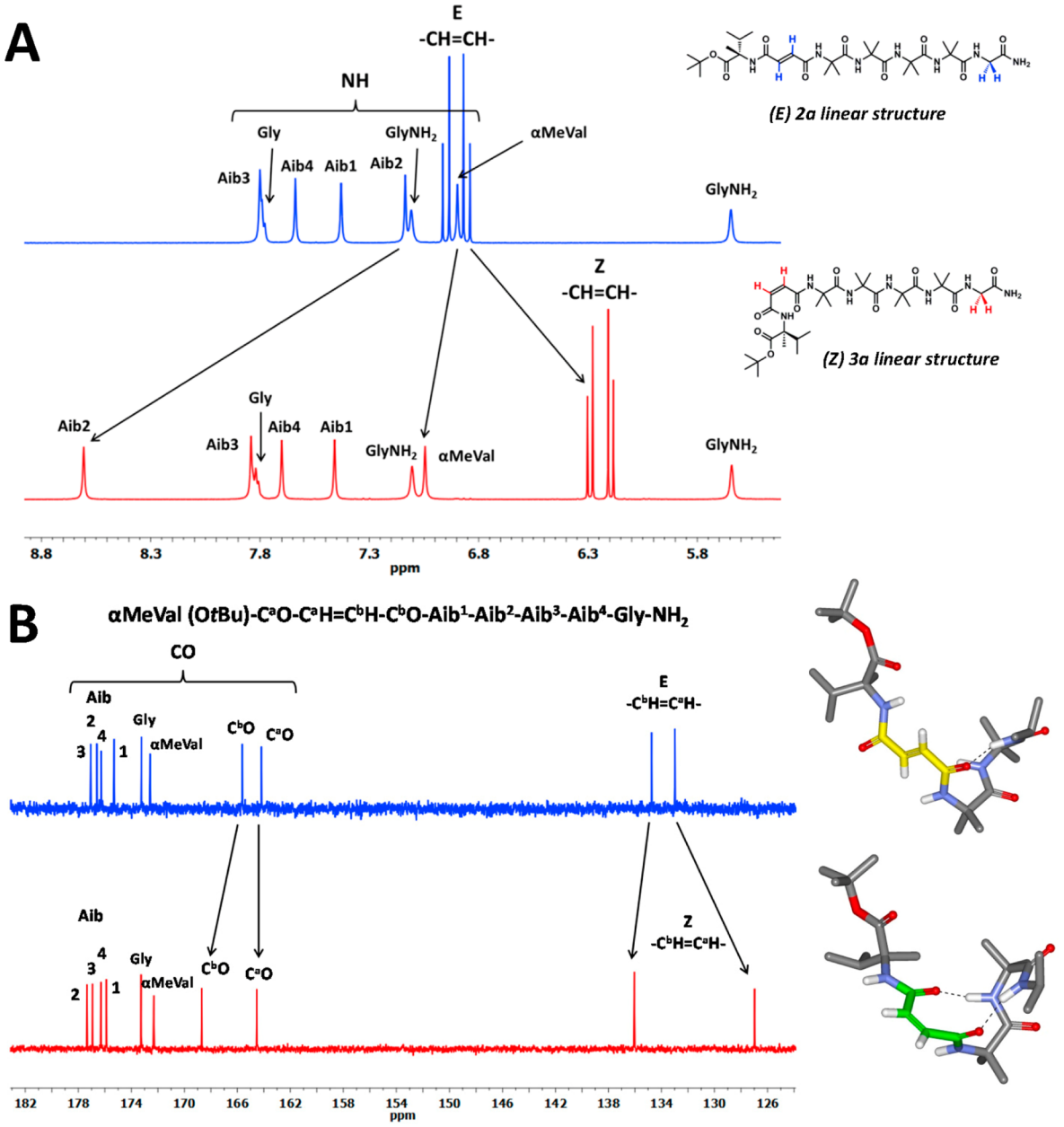

Figure 1. (A) ^{1}H NMR spectra (500 MHz in CD_3CN) and assignments showing the NH and olefinic signals of the *E* (fumaramide) isomer **2a** (blue) and *Z* (maleamide) isomer **3a** (red). (B) ^{13}C NMR spectra (500 MHz in CD_3CN) and assignments showing the carbonyl and olefinic signals of *E* (fumaramide) isomer **2a** (blue) and *Z* (maleamide) isomer **3a** (red). Right: the conformations about the fumaramide and maleamide unit, respectively, proposed for isomers **2a** and **3a**.

observation suggests that the *E* to Z photoswitch allows the involvement of the NH of Aib(2) in a new intramolecular H-bond.

Additionally, ^{13}C NMR experiments showed remarkable differences in the chemical shifts occurring for both carbonyl groups and the corresponding olefinic carbons belonging to the fumaramide or maleamide moieties (Figure 1B). In particular, for (*E*) **2a** the carbons C^bO (on the Aib side) and —C═$\underline{C}^b$— are only slightly deshielded relative to their counterparts C^aO [on the (*α*Me)Val side] and —$\underline{C}^a$═C— (Figure 1 B, upper part). Upon photoisomerization to the *Z* isomer **3a** (Figure 1 B, lower part), the C^bO signal moves significantly downfield while the position of the C^aO signal remains essentially the same as in the *E* isomer **2a**. Concomitantly, the —$\underline{C}^a$═C— in **3a** becomes much more shielded than in **2a**, whereas the —C═$\underline{C}^b$— signal moves slightly downfield. It can reasonably be expected that in the *E* configuration the fumaramide moiety adopts a planar conformation, with electronic delocalization extending from the C═C double bond as far as the nitrogen atoms on both sides (Figure 1 B, upper part). In the case of the maleamide, the large downfield shift of the C^bO signal can be ascribed to its less effective conjugation with the C═C double bond, as a result of the rotation of the C^b═O bond out of the plane of the maleamide unit. Support for this view is provided by NMR analysis of the related compounds **3c**–**3e** (see below). Since the positions of the ^{1}H and ^{13}C NMR signals of the Aib residues, apart from the NH proton signal of Aib(2), are broadly identical in **2a** and in **3a**, it can be safely assumed that the helical conformation of the -$(Aib)_4$- segment is not affected by the photoisomerization. On this basis, in the *Z* isomer **3a** the

DOI: 10.1021/jacs.6b04435
J. Am. Chem. Soc. 2016, 138, 8007–8018

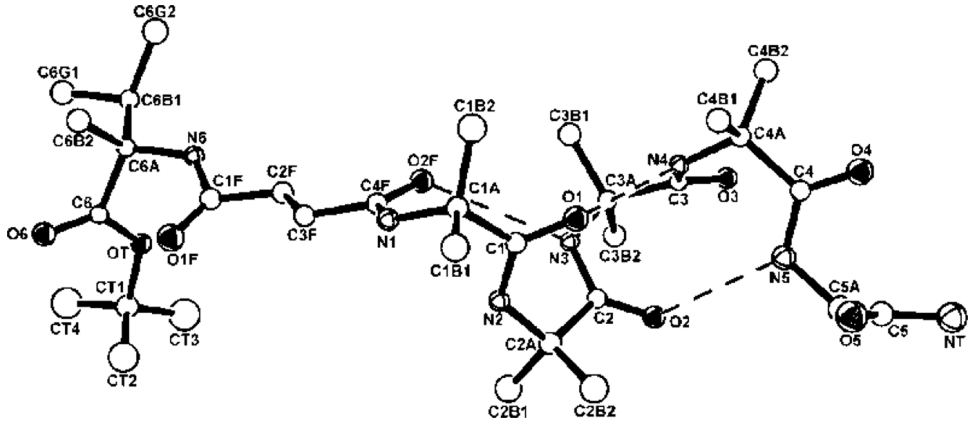

Figure 2. X-ray diffraction structure of **2a** with atom numbering. Intramolecular H-bonds are indicated by dashed lines.

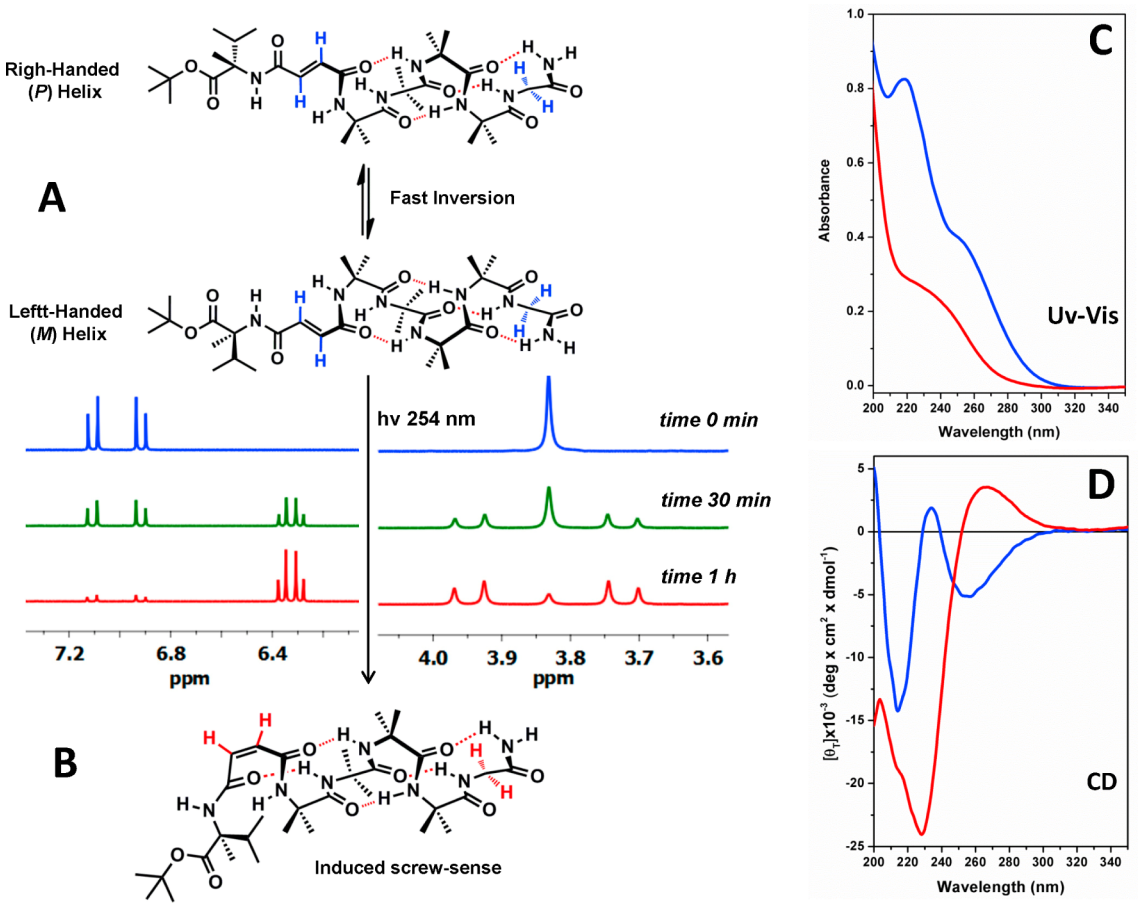

Figure 3. (A,B) Details of the ^{1}H NMR spectra of (*E*) **2a** before irradiation (blue line) and after irradiation at 254 nm for different times (30 min, green line and 1 h, red line), leading to the conversion to (*Z*) **3a**. The sample was directly irradiated in a quartz NMR tube with a 6W UV lamp. The olefinic signals (left) and the glycinamide methylene signals (right) are shown. (C) UV−vis absorption spectra of (*E*) **2a** (blue line) and (*Z*) **3a** (red line) in MeOH solution. (D) Far-UV CD spectra of (*E*) **2a** (blue line) and (*Z*) **3a** (red line) in MeOH solution (0.3 mM).

only likely acceptor of the H-bond formed by the Aib(2) NH is the carbonyl carbon of the maleamide unit adjacent to the L-(αMe)Val residue, according to the model illustrated in Figure 1 (bottom right).

The proposed conformation of the *E* isomer **2a** in solution, as inferred from the NMR data (Figure 1), is nicely corroborated by its single crystal X-ray diffraction structure (Figure 2). All of the amide and ester bonds are found in the usual *trans* disposition, none of them deviating by more than ±9.0° from the ideal *trans* planarity (180°). The conformation adopted by the L-(αMe)Val residue is right-handed helical [ϕ,ψ = −58.4(3)°, −47.9(3)°], as expected, and its isopropyl side chain is found in the common tg^{-} disposition.[39,41] The torsion angle about the double bond of the fumaric unit (C1F−C2F−C3F−C4F) is −174.6(3)°. Both fumaramide carbonyl oxygen atoms are in a *cisoid* arrangement relative to the double bond, the torsion angles O1F−C1F−C2F−C3F and C2F−C3F−C4F−O2F being −17.5(5)° and −11.4(5)°, respectively. As a result, the two oxygen atoms are slightly displaced from the average plane defined by the C1F, C2F, C3F and C4F atoms,

DOI: 10.1021/jacs.6b04435
J. Am. Chem. Soc. 2016, 138, 8007−8018

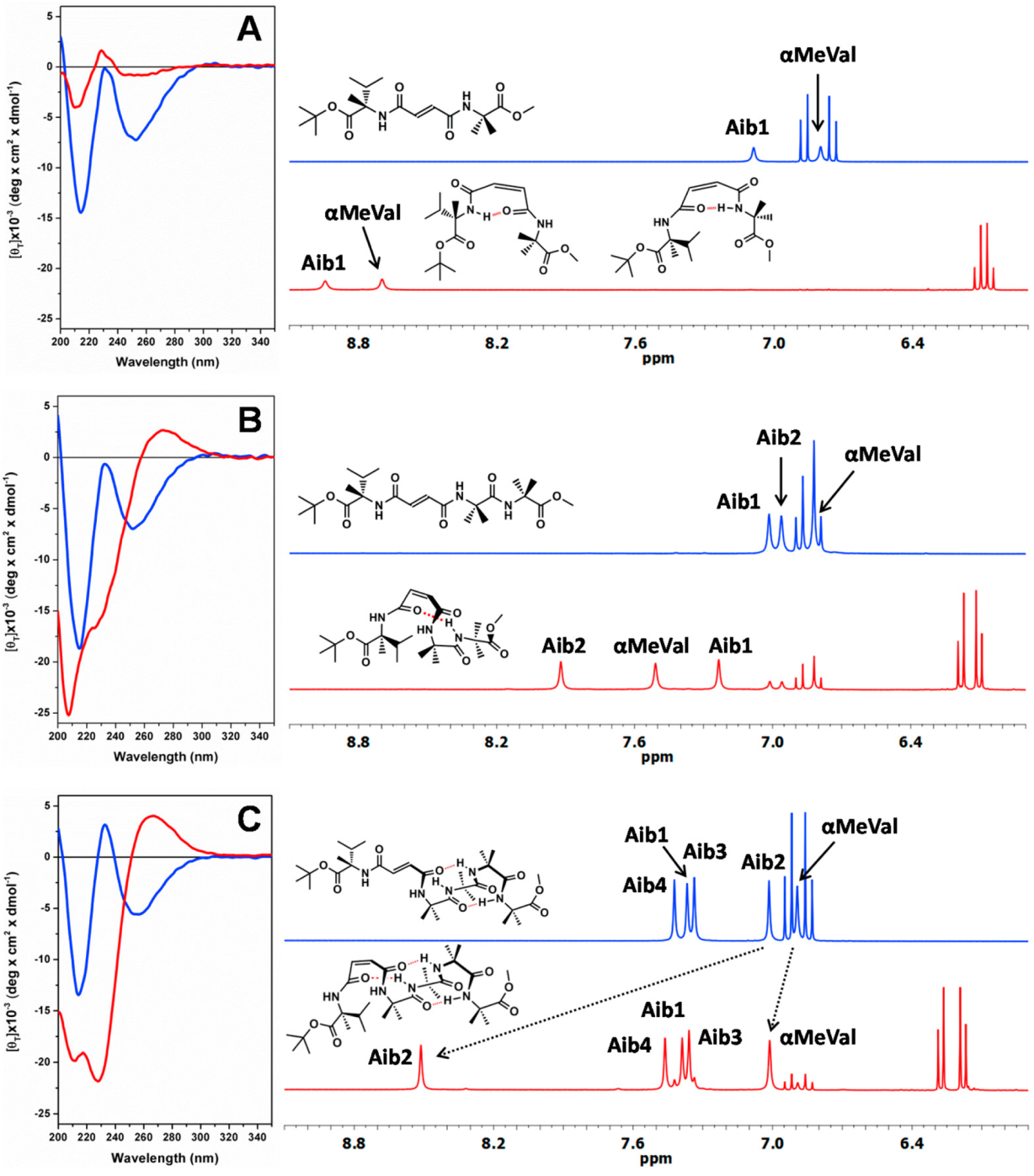

Figure 4. CD spectra (MeOH, 0.3 mM) and part of the ^{1}H NMR (500 MHz, CD_3CN) spectra of (A): (*E*) **2c** (blue line) and (*Z*) **3c** (red line); (B): (*E*) **2d** (blue line) and (*Z*) **3d** (red line); (C): (*E*) **2e** (blue line) and (*Z*) **3e** (red line).

O1F by 0.229(3) Å and O2F by 0.122(2) Å. The -$(Aib)_4$- segment is folded into a right-handed 3_{10}-helix, stabilized by four intramolecular H-bonds between the NH groups of Aib(3), Aib(4) and Gly(5) and the carbonyl oxygen atoms O2F, O1, and O2, respectively. The average values of the ϕ,ψ backbone torsion angles for the -$(Aib)_4$- segment are −55°, −32°. The C-terminal Gly residue adopts a semiextended conformation with the sign of the ϕ torsion angle opposite to that of the preceding Aib residues, with no intramolecular H-bond to the C-terminal primary amide. In the packing mode, the network of intermolecular H-bonds involves all of the potential H-bond donors that are not already intramolecularly engaged, including the C-terminal primary amide (SI, Table S3).

Despite the evident helical conformation of the -$(Aib)_4$- segment of **2a** in both the solution and solid state, the appearance of the glycine methylene signal as a singlet in the ^{1}H NMR spectrum suggests that the chiral center of the L-(αMe)Val residue induces no screw-sense preference in the Aib helix.[42,43] In the X-ray crystal structure, the distance between the C^α atoms of L-(αMe)Val and Aib(1) is 8.54 Å, with no obvious mechanism for transfer of chiral information across the fumaramide spacer to the helical -$(Aib)_4$- segment. Indeed, although in this X-ray crystal structure the -$(Aib)_4$- segment is

DOI: 10.1021/jacs.6b04435
J. Am. Chem. Soc. 2016, 138, 8007−8018

right-handed helical, a model built by reversing the sign of all torsion angles from Aib(1) to the C-terminal primary amide (SI, Figure S4) clearly shows that a left-handed helix is structurally compatible with an L-(αMe)Val residue at the other end of the fumaramide spacer. In this model, the closest distance between atoms of (αMe)Val and the -(Aib)$_4$- segment, involving a C^{γ} of (αMe)Val and a C^{β} of Aib(2), is 7.45 Å, too far to elicit any bias against a left-handed screw sense.

The inversion of double bond geometry to the *Z* (maleamide) isomer has significant consequences for the conformational preference of the -(Aib)$_4$- portion of the oligomer. Concurrent with the change in the olefinic region of the ^{1}H NMR spectrum as **2a** is converted into **3a**, the 2H singlet arising from the glycinamide methylene group splits into an AB system, with a chemical shift separation of 218 ppb. (Figure 3A,B; SI, Figure S5). Because the screw sense conformers of the Aib helix are in fast exchange on the NMR time scale, and the chiral influence is remote from the glycinamide residue, this change in chemical shift separation indicates that the level of screw sense control transmitted through the oligomer increases from zero in the *E* derivative **2a** ($\Delta\delta$ = 0 ppb) to 41% helical excess in the *Z* derivative **3a** ($\Delta\delta$ = 218 ppb) (calculated as outlined in ref 43). In other words, photoisomerization has induced *helix deracemization* by allowing stereochemical information to be communicated [probably through the proposed new hydrogen bond to Aib(2)] from the terminal chiral residue to the achiral helical domain. Similar behavior was also observed in the glycinamide signals of the longer oligomer **2b**, which indicated no helical screw-sense preference (0% h.e.), and **3b**, in which a chemical shift separation $\Delta\delta$ = 145 ppb indicated a helical excess of 27% (SI, Figure S6), measured at the glycinamide terminus.

Peptides **2a** and **3a** were further characterized using UV−vis absorption and CD measurements in MeOH solution (Figure 3). The UV−vis spectra of **2a** and **3a** show distinctively different profiles, with strong contributions from absorption bands attributed to $\pi \rightarrow \pi^*$ transitions of the fumaramide/maleamide conjugated systems.[45] Compound **2a** displays a more intense UV−vis profile with an absorption maximum at 200 nm and a pronounced shoulder at about 260 nm (Figure 3C). With regard to far-UV CD analyses, the *E* isomer **2a** exhibit a moderately intense negative maximum at 212 nm followed by two weak bands of opposite sign, positive at 238 nm and negative at 255 nm (Figure 3D, blue line). A very different CD profile is shown by the *Z* isomer **3a** (Figure 3D, red line), characterized by an intense negative maximum at 228 nm (with a shoulder at 212 nm) followed by a weak positive maximum at 265 nm.

An ^{1}H 1D- and 2D-NMR (NOESY) investigation was performed for the series of *E*-configured oligo-Aib peptide methyl esters **2c−f** and their *Z* isomers **3c−f** in CD_3CN. From a comparison of the ^{1}H NMR spectra, we found a number of variations in the chemical shifts of the NH signals upon photoisomerization (Figure 4). In the case of the shortest compounds **2c** and **3c**, both NH [Aib and (αMe)Val] signals appear at higher chemical shift in the spectrum of the *Z* isomer **3c** (Figure 4A). Similar behavior was observed for **2d** and **3d** but the variation of chemical shift was less pronounced (Figure 4B). The spectra of **2e** and **3e** resemble in shape those of **2a** and **3a**, in which only the Aib(2) and (αMe)Val NH signals revealed significantly different chemical shifts (Figure 4C). Additional information was obtained from the NOESY spectra (SI, Figures S10−S12). We found sequential connectivities $\beta CH_3(i) \rightarrow \alpha NH(i+1)$ in the NOESY spectra of **2d** (Aib^1 → Aib^2) and **2e** (Aib^1 → Aib^2, Aib^2 → Aib^3). All sequential $\alpha NH(i) \rightarrow \alpha NH(i+1)$ connectivities are visible in the NOESY spectra of peptides **2e**/**3e**, confirming the presence of a well-developed helical conformation throughout the -(Aib)$_4$- segment (SI, Figure S12).

The intriguing behavior of the NH proton signals of the maleamide derivatives on increasing the chain length of the peptide (^{1}H NMR spectra of compounds **3c**, **3d**, and **3e** in Figure 4 and **3a** in Figure 1) merits detailed analysis. In this type of compound, carrying two secondary amides adjacent to the C=C double bond, a planar arrangement in which both carbonyl oxygens of the maleamide unit are *cisoid* to the double bond (*cZc* conformation) is sterically forbidden. Indeed, DFT calculations[45] on the simple model system (*Z*) CH_3—NH—CO—CH=CH—CO—NH—CH_3 suggested that the most stable conformation is planar but characterized by the dispositions of one carbonyl oxygen *cisoid* and the other *transoid* to the double bond (*cZt* or *tZc* conformations), which allows the formation of a rather strong intramolecular H-bond between the carbonyl oxygen of one amide and the NH group of the other, thus leading to a significant downfield shift of the NH proton signal. Such a conformation, in which the H-bond closes a planar ring of seven atoms, was authenticated by X-ray diffraction for symmetrically substituted (secondary) maleamides.[46,47] We eventually succeeded in growing a single crystal of compound **3c** and solving its structure by X-ray diffraction analysis. All of the five independent molecules composing the asymmetric unit (one of them is illustrated in Figure 5) adopt

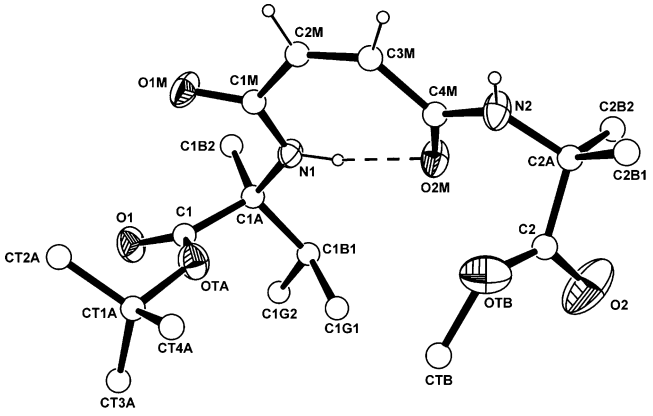

Figure 5. X-ray diffraction structure of **3c**. One of the five conformationally similar independent molecules composing the asymmetric unit is shown, with atom numbering. H atoms are in part omitted for clarity. The intramolecular H-bond is represented by a dashed line.

similar conformations, and feature an intramolecular H-bond between the NH group of (αMe)Val and the maleamide carbonyl oxygen preceding the Aib residue. The N···O and H···O separations are in the ranges 2.706(5)−2.746(6) Å and 1.89−1.93 Å, respectively, and the N−H···O angles are within 155−159°. In this conformation, the maleamide carbonyl next to (αMe)Val is *transoid* to the double bond [the O1M-C1M-C2M-C3M torsion angle is 168.4(7)°], whereas the maleamide carbonyl oxygen preceding the Aib residue is *cisoid* [C2M−C3M−C4M−O2M torsion angle 15.1(11)°]. Such a conformation about the maleamide unit can be designated as *tZc*, where the leftmost letter refers to the disposition of the carbonyl oxygen closer to the (αMe)Val residue. In solution,

DOI: 10.1021/jacs.6b04435
J. Am. Chem. Soc. 2016, 138, 8007−8018

the two carbonyl oxygens might exchange their dispositions [that on the (αMe)Val side from *transoid* to *cisoid*, and that on the Aib side from *cisoid* to *transoid*], leading to an alternative conformation (*cZt*) in which the Aib NH would be intramolecularly H-bonded while the (αMe)Val NH would be free. If these two conformations interconvert rapidly on the NMR time scale, both NH signals are expected to resonate at relatively low field. This is indeed what we observe in the ^{1}H NMR spectrum of **3c**, in which the NH proton signals of (αMe)Val and Aib are found at δ 8.70 and 8.94, respectively. As the peptide chain is elongated to $(Aib)_2$ in **3d** and to $(Aib)_4$ in **3e**, the (αMe)Val and Aib(1) NH signals move upfield relative to those of **3c** (to δ 7.51 and 7.23, respectively, for **3d**, and to δ 7.01 and 7.39, respectively, for **3e**). These findings suggest that both of the intramolecularly H-bonded conformations (*tZc* and *cZt*) proposed for **3c** become less populated on lengthening the Aib chain. Instead, a new conformation in which the Aib(2) NH is strongly intramolecularly H-bonded (as its NH signal is found at δ 7.92 for **3d**, and at δ 8.51 for **3e**) seems to progressively emerge.

To clarify this issue, we built molecular models of **3e** combining the *tZc* or the *cZt* planar conformations of the maleamide unit and the right-handed or left-handed helical conformations of the $(Aib)_4$ segment (Figure 6). The L-(αMe)Val residue was kept in the right-handed helical conformation. We found that the combinations of the *tZc* conformation [in which the (αMe)Val NH is H-bonded to the maleamide carbonyl next to Aib(1)] with either a right-handed or left-handed helical $(Aib)_4$ segment are highly disfavored by severe steric clashes between the entire (αMe)Val isopropyl side chain (including the C^β atom) and the Aib(3) residue (Figure 6A,B). Combinations of the *cZt* conformation [in which the Aib(1) NH is H-bonded to the maleamide carbonyl next to (αMe)Val] with a right-handed or a left-handed helical $(Aib)_4$ segment seem to be less unfavorable, but still display relatively short contacts (C···C distances about 3.7−3.8 Å) between one of the CH_3 groups of the O*t*Bu moiety with either both the βCH_3 groups of Aib(2) (for the right-handed helix) or the *pro-R* βCH_3 of Aib(1) (for the left-handed helix). However, these interactions (illustrated in Figure 6C,D) can be relaxed by rotating the *t*Bu group by about 20° out of the (commonly adopted) staggered disposition relative to the COO ester moiety. These models may account for the decreasing population of conformations containing an intramolecular H-bond to the maleamide unit [involving as the donor either the (αMe)Val or the Aib(1) NH group] as the Aib chain is elongated.

On the basis of the NMR evidence, the prevailing conformer for **3e** might be similar to that adopted by **3a** (schematically outlined in Figure 1), characterized by the involvement of the Aib(2) NH in an intramolecular hydrogen bond, while preserving a 3_{10}-helical conformation in the -$(Aib)_4$- segment. The only likely acceptor of an intramolecular hydrogen bond from the Aib(2) NH is the maleamide carbonyl oxygen adjacent to the (αMe)Val residue. To allow formation of such a hydrogen bond, the maleamide unit must adopt a twisted *cZc* conformation, in which the maleamide C═O group next to Aib(1) is rotated out of the C—CH═CH—C plane, and the associated C═C—C═O torsion angle must be close to either +60° or −60°, depending on whether the following peptide helix is right-handed or left-handed. An example of a similar *cZc* arrangement, twisted by as much as 76°, has been reported for a tertiary maleamide.[48] If the maleamide system is significantly

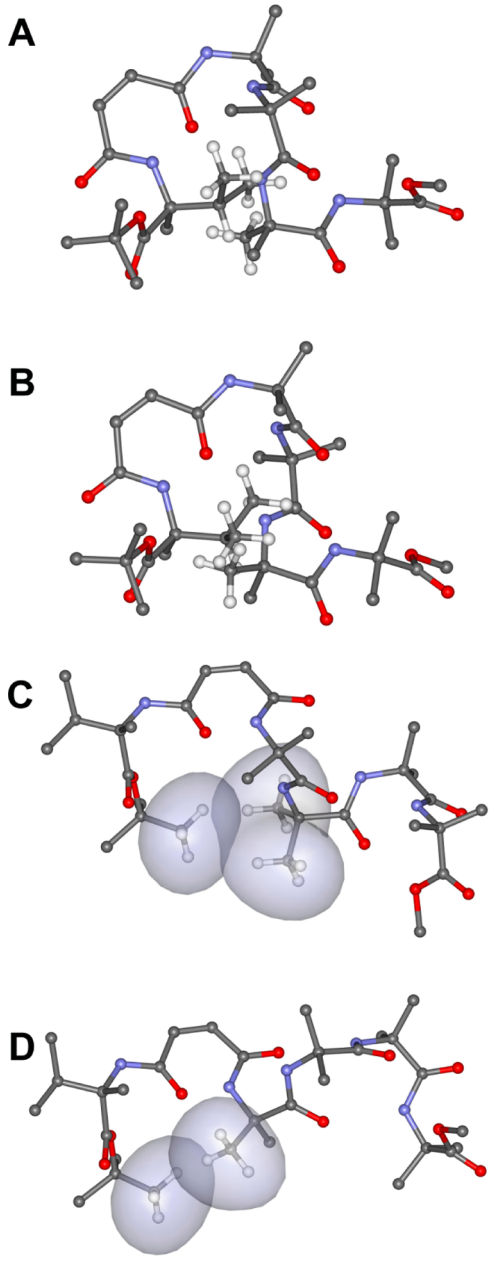

Figure 6. Models of compound **3e** built by combining either the *tZc* or *cZt* disposition about the maleamide moiety with a right-handed or left-handed 3_{10}-helical conformation of the -$(Aib)_4$-OMe segment: (A) *tZc* and right-handed helix; (B) *tZc* and left-handed helix; (C) *cZt* and right-handed helix; (D) *cZt* and left-handed helix. In A and B, the H atoms on the (αMe)Val isopropyl side chain and the *pro-R* βCH_3 of Aib[3], involved in steric clashes, are shown. In C and D, the van der Waals surfaces of the groups involved in short contacts are highlighted.

twisted on the Aib side while essentially planar on the (αMe)Val side, then the distance between the Aib(1) NH proton and the proximal olefinic CH proton must be larger than the corresponding distance on the (αMe)Val side. The different intensities of the related NH−CH cross-peaks in the NOESY spectrum of **3e** (SI, Figure S12, panel D) support this hypothesis. Molecular models suggest that when the oligo-Aib 3_{10}-helix is left-handed and the twist about the maleamide C═C—C═O torsion angle is negative (Figure 7A), there are no significant unfavorable interactions between the helix and the L-(αMe)Val-O*t*Bu residue, apart from a short contact (C···C

DOI: 10.1021/jacs.6b04435
J. Am. Chem. Soc. 2016, 138, 8007−8018

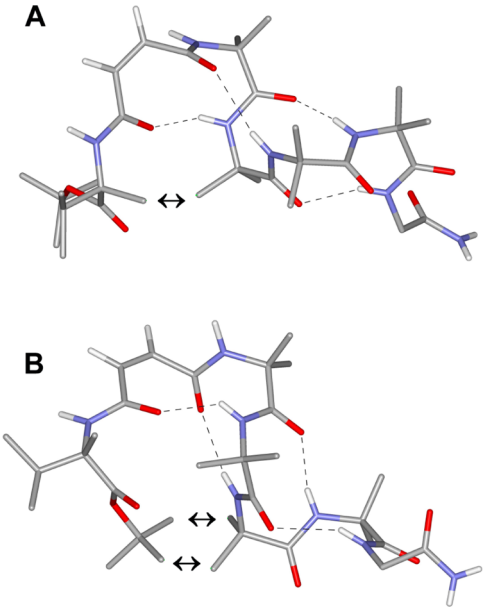

Figure 7. Models of compound **3a** combining: (A) a negative twist about the maleamide C═C—C═O torsion angle on the Aib side and a left-handed 3_{10}-helix, and (B) a positive twist about the maleamide C═C—C═O torsion angle on the Aib side and a right-handed 3_{10}-helix. Intramolecular H-bonds are indicated by dashed lines. The short C···C contacts are highlighted.

distance 3.3 Å) between the (αMe)Val β-CH_3 group and the *pro-R* βCH_3 of Aib(2). Conversely, the combination of a positive twist about the maleamide C═C—C═O torsion angle and a right-handed helix brings the O*t*Bu group too close to the βCH_3 groups of Aib(3) (Figure 7B). For the O*t*Bu rotamer [eclipsing the C(═O)—O bond] with the least crowding of Aib(3), the C···C distances between CH_3 groups of the O*t*Bu moiety and of the Aib(3) residue are about 2.4 Å. Unfortunately, extensive signal overlap in the CH_3 region of the NOESY spectra of **3a** and **3e** prevented us from extracting additional information in support of our hypotheses. In addition, despite extensive effort, we were unable to grow single crystals of **3a** or **3e** suitable for an X-ray diffraction analysis. The tentative models outlined above suggest that the prevailing screw sense of the peptide helix of the (*Z*) isomers **3a** and **3e** is left-handed.

In order to characterize the influence of possible contributions of peptide domains, in addition to the fumaramide/maleamide chromophores, on the CD spectra of **2a** and **3a**, we extended the CD study to the series of *E*-configured oligo-Aib peptide methyl esters **2c**−**f** and their *Z* isomers **3c**−**f**. The CD spectrum of *E* derivative **2c** is similar to those of *E* isomers **2a** and **2b**, while the CD spectrum of *Z* **3c** is comparable in profile to that of its *E* isomer **2c**, but much weaker (Figure 4A). The CD spectra of the *E* compounds **2d**−**f** are similar to the spectra of both **2a**,**b** and the nonhelical homologue **2c** (Figure 4B,C; for CD spectra of compounds **2f** and **3f** see SI). The *Z* isomers **3d**−**f** provided more interesting information. In the case of **3d** (with two Aib residues, Figure 4B) the spectrum, while resembling those of **3a**,**b**, shows intriguing features. A negative maximum at 208 nm is followed by a pronounced shoulder at 227 nm and a positive maximum at 270 nm. The CD spectrum of **3e** (with four Aib residues; Figure 4C) shows two intense negative maxima of similar intensity at 209 and 228 nm, again with a positive maximum at 260−270 nm. Finally, compound **3f** (with eight Aib residues; SI, Figure S9) displays a CD signature almost superimposable upon the curve shown by **3b**. Overall, the CD spectra of all of these compounds appear to be dominated by bands related to electronic transitions of the fumaramide/maleamide chromophores which become CD-active owing to the proximity of the chiral L-(αMe)Val residue. While extension of the oligo-Aib chain has little effect on the CD spectra of the *E* isomers, the CD spectra of the *Z* isomers show pronounced changes as a function of the length of the oligo-Aib chain. This behavior may be partly explained by differences in the relative populations of the *cZt*, *tZc*, and distorted *cZc* conformers about the maleamide unit for the different members of this set of compounds, as suggested by their NMR analyses (see above). The CD spectrum of a 3_{10}-helix is characterized by maxima (negative for a right-handed helix) at 222 and 207 nm, with intensity ratio of about 0.4.[38] In principle, for the longest *Z* isomers, a contribution to the CD profile from a helical oligo-Aib domain of one prevailing screw sense cannot be ruled out. However, our results do not allow us to assign unambiguously a right- or left-handed screw sense preference to this oligo-Aib helix. Furthermore, while the shortest compounds **2c** and **3c** undergo *E* to *Z* reversible isomerization under irradiation at 254 nm (65% yield, CD_3CN solution) or 312 nm (55% yield, $CDCl_3$ solution) respectively[45] (see SI), for compounds **3a**,**b**, **3d**−**f** the isomerization from *E* to *Z* yields almost quantitatively the maleamide form. This feature is surprisingly enough and tentatively, driven by the formation of a novel intramolecular H-bond. The isomerization from *Z* to *E* was not possible in all of these last compounds, due to the overlapping of the UV-absorption profiles of the *E* and *Z* isomers in the 290−330 nm region, possibly related in our case to the "unusual" conformation of the maleamide form.

Photoswitchable Stereoselection. Having established that photoisomerisation of the *E* fumaramide unit to the *Z* maleamide brings the chiral L-(αMe)Val residue into sufficiently close contact with the oligo-Aib domain for it to induce a preferred screw sense, the next challenge was to use this induced preference to achieve a measurable chemical output. Achiral helices of preferred screw sense have been used to mediate the remote transmission of stereochemical information to reactive sites,[26] and we have reported the use of light to invert the enantioselectivity induced by a catalytic site.[21] Secondary structure plays a key role in the enantioselective chain extension reactions of helical peptides,[49−51] and induction of a globally chiral secondary structure in an achiral peptide chain by a single remote chiral residue at the N terminus is on its own sufficient to allow enantioselective chain extension at the C terminus.[51] To demonstrate the potential of a system in which diastereoselectivity dependent on a helical screw sense preference can be turned on or off using light, 5(*4H*)-oxazolones (azlactones) were formed from the tetra- and octa-Aib peptides **2e** and **2f**. These were hydrolyzed under basic conditions to the corresponding *E*-configured carboxylic acids **4a**,**b** (Scheme 2; see SI for details). The corresponding (*Z*) isomers **5a**,**b** were easily formed by irradiation with UV light. The peptide oxazolones **6a**,**b**, **7a**,**b** were synthesized by reaction with EDC in an appropriate solvent. To run the diastereoselection experiments, the oxazolones **6a**,**b** and **7a**,**b** were allowed to react with a large excess (8 equiv) of H-D,L-Val-OMe (Scheme 2 and Figure 8A). Pairs of diastereomers were formed in ratios that were quantified by reverse phase HPLC. An initial set of experiments

DOI: 10.1021/jacs.6b04435
J. Am. Chem. Soc. 2016, 138, 8007−8018

Scheme 2. Synthesis of the Peptide Oxazolones 6a,b and 7a,b and Their Exploitation in the Diastereoselective Formation of 8a–d and 9a–d

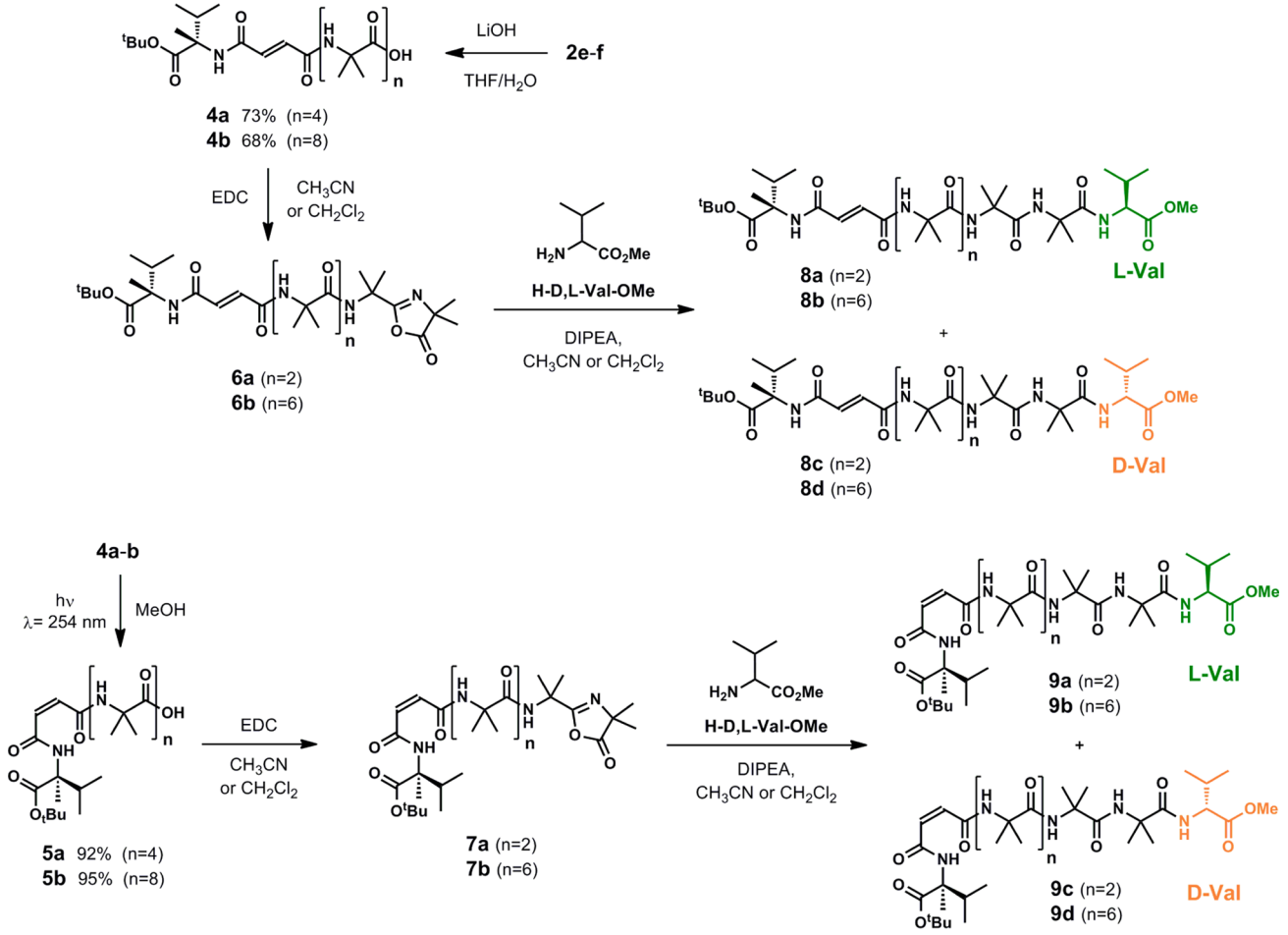

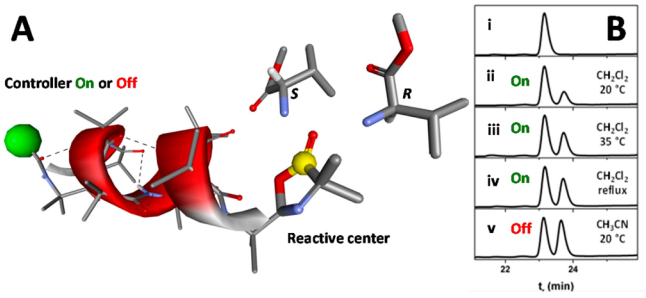

Figure 8. (A) Schematic representation of the diastereoselective chain extension reactions performed by treating H-D,L-Val-OMe with peptide oxazolones carrying a chiral L-(αMe)Val-O*t*Bu moiety connected through a photoswitchable fumaramide (*E*) or maleamide (*Z*) linker to a helical oligo-Aib domain. (B) HPLC traces of (i) an authentic sample of (*Z*) **9b**; (ii) reaction mixture of **7b** with H-D,L-Val-OMe in CH_2Cl_2 at 20 °C, at (iii) 40 °C and (iv) under reflux; (v) reaction mixture of **7b** with H-D,L-Val-OMe in CH_3CN at 20 °C.

was performed in acetonitrile at different temperatures (20, 40 and 70 °C). In no case was stereoselectivity observed: for both *E* and *Z* geometrical isomers of the reactant peptide oxazolones (**6a**/**7a**, **6b**/**7b**) the pairs of diastereomeric products (**8a**/**c** or **8b**/**d**, **9a**/**c** or **9b**/**d**) were formed in a 50:50 ratio. The reactions were repeated in CH_2Cl_2 (at 20 °C, 35 °C and under reflux). Again, no stereoselectivity was detected in the reactions involving the *E* isomers **6a,b** and the short-chain (*Z*) **7a**. Conversely, in CH_2Cl_2 the (*Z*) **7b** isomer, characterized by an -(Aib)$_7$- domain preceding the oxazolone moiety, showed remarkable stereoselectivity in a chain extension reaction, incorporating preferentially L-Val-OMe (Figure 8B). As shown in Table 1, lower temperatures increased the diastereoselectivity of the reaction, up to a 74:26 ratio of the diastereomeric products at 20 °C.

Table 1. Diastereoselective Chain Extension Reactions of the Peptide Oxazolone (*Z*) 7b with H-D,L-Val-OMe[a]

solvent	temperature	**9b**:**9d**
CH_2Cl_2	20 °C	74:26
CH_2Cl_2	35 °C	62:38
CH_2Cl_2	reflux	57:43
CH_3CN	20 °C	51:49
CH_3CN	40 °C	50:50
CH_3CN	70 °C	50:50

[a]The diastereoisomeric ratio **9b**:**9d** was determined by HPLC.

These findings are in agreement with previous reports that low polarity solvent and low temperature markedly favor higher stereoselectivity in chain extension reactions using racemic amino acid monomers.[52] The effect of solvent on the stereoselectivity may be tentatively rationalized as follows. As a results of cooperative effects, the extent to which *N*-acylated Aib homo-oligopeptide esters populate the 3_{10}-helical con-

DOI: 10.1021/jacs.6b04435
J. Am. Chem. Soc. 2016, 138, 8007–8018

Scheme 3. Synthesis of 12 and Isomerization to Its Maleamide Isomer 13

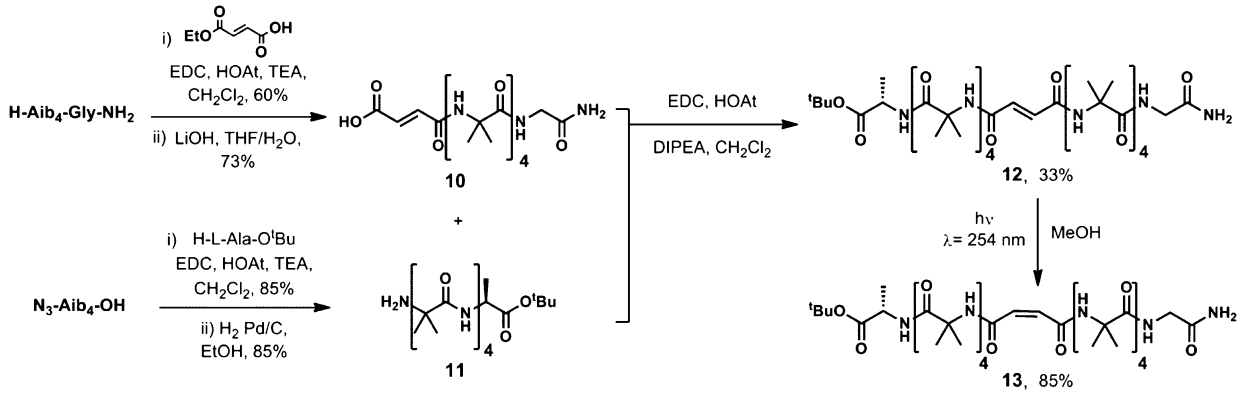

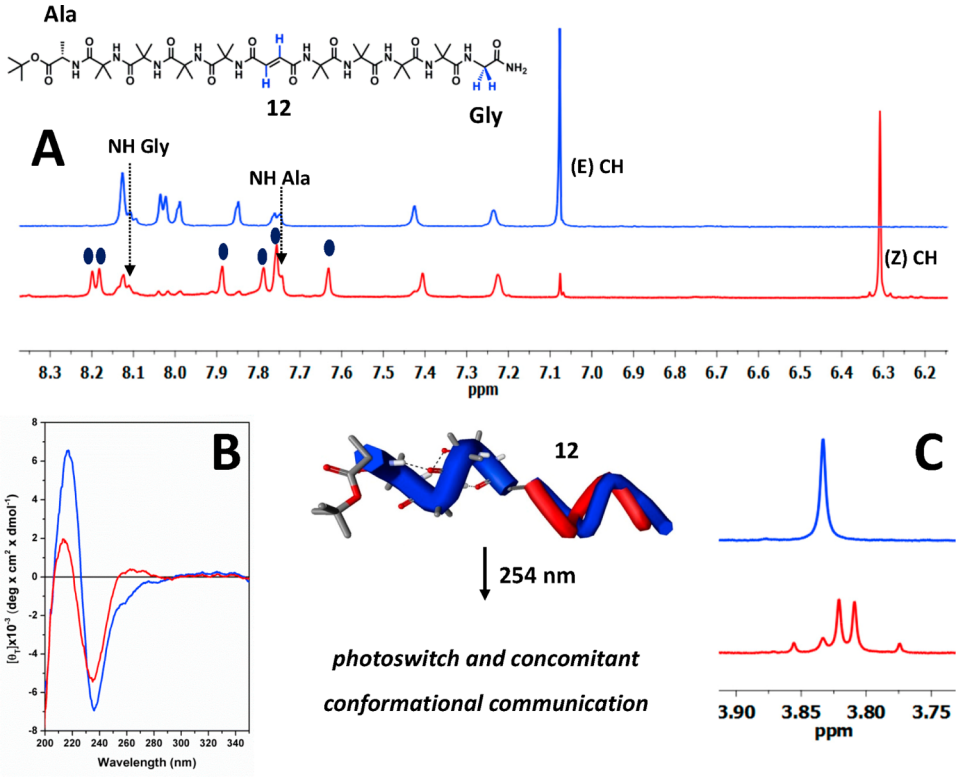

Figure 9. (A) Details of the ^{1}H NMR spectra (500 MHz, CD_3OH) of (*E*) **12** (blue) and (*Z*) **13** (red), showing NH and olefinic signals. (B) CD spectra of **12** (blue) and **13** (red) in MeOH solution. (C) Detail of the ^{1}H NMR spectra (500 MHz, CD_3OD) of **12** (blue) and **13** (red) showing the glycinamide methylene signals.

formation depends on the maximum number of intramolecular hydrogen-bonds (C_{10} structures) that can be formed at a given main-chain length, ranging (in $CDCl_3$ solution) from 41% and 69% for tri- and tetrapeptides to nearly 100% for octapeptides.[53,54] Thus, greater levels of fully developed or incipient helical conformations can be expected for the longer oligomer **7b** than the shorter oligomer **7a** in CH_2Cl_2 solution. Although its higher polarity lessens the screw sense fidelity in Aib-based peptides,[27] helical conformations are still prevalent in CH_3CN[27,37,43] (as confirmed by our NMR results from **3a**), so the lack of diastereoselectivity in the reaction of **7b** with racemic H-D,L-Val-OMe in CH_3CN cannot be ascribed to the lack of transfer of chiral information from L-(αMe)Val to the peptide helix but rather a local reduction of selectivity at the C-terminal oxazolone. As the transition state of the most likely reaction path of peptide bond formation via oxazolones is reactant-like,[50] conformational information on peptide oxazolones might be relevant to the stereochemical outcome of the reaction. The crystal structures of peptide oxazolones in which the residue preceding the ring is Aib or a conformationally similar C^{α}-tetrasubstituted α-amino acid point to a strongly preferred disposition of the oxazolone ring,[51,55−61] that allows the onset of C−H···O and/or C−H···N hydrogen bonds between the βCH_3 groups of the preceding residue and the ring heteroatoms.[57] It is likely that these weak interactions[62] stabilize the disposition of the oxazolone relative to the helical domain more effectively in CH_2Cl_2 than in CH_3CN.

It remains to be established whether the diastereoselectivity arises from a prevailing right- or left-handed screw sense in the helical oligo-Aib domain. Diastereoselective reactions of oxazolone derivatives of 3_{10}-helical L-(αMe)Val homo-oligomers, Ac-[L-(αMe)Val]$_n$-OXL (n = 4−8) with racemic

DOI: 10.1021/jacs.6b04435
J. Am. Chem. Soc. 2016, 138, 8007−8018

H-D,L-Val-OMe indicated that right-handed helices preferentially incorporate D-Val-OMe.[51] Conversely, EDC/HOBt mediated chain extension of Aib oligomers, induced to adopt a right handed screw sense by a remote L-(αMe)Val residue, preferentially incorporate L-Val-OMe.[52] Chain extension of peptide oxazolone **7b** led to preferential incorporation of L-Val-OMe, but it is not possible to use this result to deduce unequivocally the prevailing screw sense of the helical Aib domain.

Helix-to-Helix Communication. The ability of peptide domains of defined secondary structure to influence each other's conformation is crucial to the function of allosteric enzymes and other switchable proteins such as membrane-bound receptors. Communication between foldamer domains has been explored in both amide[63] and urea[64] series. The fumaramide/maleamide switch opens the possibility that conformational communication between helical peptide domains might be modulated by light. We investigated such a system, in which the photoswitchable linker serves as a means of conducting or insulating conformational communication between two helical Aib_4 domains linked head-to-head (N-terminus to N-terminus) (Scheme 3). A chiral inducer (L-Ala-O*t*Bu) and a glycinamide NMR reporter were each located at the C-terminus of the two Aib_4 domains. L-Ala can participate in a 3_{10} helical structure, and as its ester derivative it induces high levels of left-handed screw-sense control when located at the C-terminus of an Aib oligomer.[65] Monoethyl fumarate was coupled to the N-terminus of H-Aib_4GlyNH$_2$ and the free carboxylic acid **10** was recovered after basic hydrolysis (Scheme 3). H-L-Ala-O*t*Bu was coupled at the C-terminus of N_3-$(Aib)_4$-OH; catalytic hydrogenation yielded **11**. Compound **12**, in which two helical pentapeptide domains are joined N terminus to N terminus through a fumaramide linker, was obtained by coupling the two fragments **10** and **11**. Fumaramide (*E*) **12** was converted to its corresponding maleamide (*Z*) isomer **13** in 85% selectivity by irradiation with UV light at 254 nm.

Comparison of the ^{1}H NMR spectra of **12** and **13** in MeOH-d_3 (Figure 9A, blue and red line respectively) reveals that while the NH signals of Ala and Gly are located at similar chemical shifts in both isomers, the shift of most of the other NH signals differs, suggesting that photoisomerization affects the hydrogen-bonding network involving the Aib residues, perhaps to a larger extent than that observed for **2a** and **3a**. Although the only stereogenic center (Ala) is separated by four Aib residues from the fumaramide (in **12**) or maleamide (in **13**) unit, it is able to elicit a significant CD signal in these two chromophores (Figure 9B), probably as the result of the left-handed helical screw sense induced in the $(Aib)_4$ domain. The CD spectrum of (*E*) **12** is characterized by two maxima of opposite sign (positive at 212 nm, and negative at 235 nm) and similar intensity. In the CD spectrum of the *Z* isomer **13** (after irradiation) the positive band around 210 nm is markedly less intense than in the corresponding *E* isomer **12**, while the intensity of the negative band around 235 nm is only slightly modified. This is consistent with left-handed screw-sense induction from the L-Ala terminus reaching at least as far as the unsaturated residue (λ_{max} = 235 nm) in both cases. Figure 6C shows the details of ^{1}H NMR spectra of **12** illustrating the signals due to the glycinamide methylene group before (blue) and after (red) irradiation at 254 nm. The singlet evident in *E* isomer **12** indicates no induction of screw sense preference at the glycinamide residue, but the chemical shift separation $\Delta\delta$ = 31 ppb of the AB system arising from *Z* isomer **13** indicates that the maleamide allows conformational information from the left-handed helical domain adjacent to the L-Ala residue to induce a screw sense preference in the more remote helical domain carrying the Gly residue. Despite this, the CD signal of *Z*-**13** is *less* intense than that of **12**. This suggests that in the case of **13** the screw sense induced in the remote helical domain is of opposite chirality to that in the domain adjacent to the L-Ala residue. The structural differentiation between the two helical domains is slight (L-Ala vs Gly), so two helices of opposite screw-sense result in an almost *meso* structure, and consequently the (*Z*) **13** isomer has a less intense CD spectrum.

CONCLUSIONS

The introduction of photoswitchable linkers into foldamers allows their conformational properties to be modulated by irradiation. Photosensitive fumaramide/maleamide linkers are particularly compatible with the hydrogen-bonded structures of peptide foldamers, with the *Z* maleamide geometry allowing hydrogen bonding across the unsaturated linker that is not possible in the *E* fumaramide configuration. The switch from the (conformationally insulating) fumaramide to the (conformationally conducting) maleamide allows chemical function, in this case stereoselectivity, to be turned on, providing a chemical analogue of a photodiode, in which light turns on *electronic* communication. In future this feature could provide a valuable structural element for the design of functional foldamers in which biomimetic function may be induced photochemically.

ASSOCIATED CONTENT

Supporting Information

The Supporting Information is available free of charge on the ACS Publications website at DOI: 10.1021/jacs.6b04435.

Crystallographic data for compounds **2a**. (CIF)
Crystallographic data for compounds **3c**. (CIF)
Full experimental details, ^{1}H and ^{13}C NMR spectra. (PDF)

AUTHOR INFORMATION

Corresponding Authors

*j.clayden@bristol.ac.uk
*alessandro.moretto.1@unipd.it

Notes

The authors declare no competing financial interest.

ACKNOWLEDGMENTS

The work was funded by the ERC (Advanced Grant ROCOCO), EPSRC (Grant EP/K039547) and the Italian Ministero dell'Istruzione, dell'Università e della Ricerca (MIUR) (program PRIN 2010NRREPL_009).

REFERENCES

(1) Armitage, J. P.; Hellingwerf, K. J. *Photosynth. Res.* **2003**, *76*, 145−155.
(2) Briggs, W. R.; Olney, M. A. *Plant Physiol.* **2001**, *125*, 85−88.
(3) Feuda, R.; Hamilton, S. C.; McInerney, J. O.; Pisani, D. *Proc. Natl. Acad. Sci. U. S. A.* **2012**, *109*, 18868−18872.
(4) Land, M.; Nilsson, D. E. *Animal Eyes*; Oxford Univ. Press: Oxford, U.K., 2002.
(5) Wald, G. *Science* **1968**, *162*, 230−239.

DOI: 10.1021/jacs.6b04435
J. Am. Chem. Soc. 2016, 138, 8007−8018

(6) Zhou, X. E.; Melcher, K.; Xu, H. E. *Acta Pharmacol. Sin.* **2012**, *33*, 291−299.
(7) Ernst, O. P.; Lodowski, D. T.; Elstner, M.; Hegemann, P.; Brown, L. S.; Kandori, H. *Chem. Rev.* **2014**, *114*, 126−163.
(8) Hubbell, W. L.; Altenbach, C.; Hubbell, C. M.; Khorana, H. G. *Adv. Protein Chem.* **2003**, *63*, 243−290.
(9) De Grip, W. J.; Rothschild, K. J. In *Molecular Mechanisms of Visual Transduction*; Stavenga, D. G., De Grip, W. J., Pugh, E. N., Jr., Eds.; Elsevier: Amsterdam, 2000; pp 1−54.
(10) Broichhagen, J.; Trauner, D. *Curr. Opin. Chem. Biol.* **2014**, *21*, 121−127.
(11) Krauss, U.; Drepper, T.; Jaeger, K.-E. *Chem. - Eur. J.* **2011**, *17*, 2552−2560.
(12) Velema, W. A.; Szymanski, W.; Feringa, B. *J. Am. Chem. Soc.* **2014**, *136*, 2178−2191.
(13) Gellman, S. H. *Acc. Chem. Res.* **1998**, *31*, 173−180.
(14) Hill, D. J.; Mio, M. J.; Prince, R. B.; Hughes, T. S.; Moore, J. S. *Chem. Rev.* **2001**, *101*, 3893−4012.
(15) Huc, I. *Eur. J. Org. Chem.* **2004**, *2004*, 17−29.
(16) Hecht, S.; Huc, I. *Foldamers: Structure, Properties and Applications*; Wiley-VCH: Weinheim, 2007.
(17) Saraogi, I.; Hamilton, A. D. *Chem. Soc. Rev.* **2009**, *38*, 1726−1743.
(18) Juwarker, H.; Suk, J.-M.; Jeong, K.-S. *Chem. Soc. Rev.* **2009**, *38*, 3316−3325.
(19) Le Bailly, B. A. F.; Clayden, J. *Chem. Commun.* **2016**, *52*, 4852−4863.
(20) Yu, Z.; Hecht, S. *Chem. Commun.* **2016**, *52*, 6639−6653.
(21) Le Bailly, B. A. F.; Byrne, L.; Clayden, J. *Angew. Chem., Int. Ed.* **2016**, *55*, 2132−2136.
(22) De Poli, M.; Zawodny, W.; Quinonero, O.; Lorch, M.; Webb, S. J.; Clayden, J. *Science* **2016**, *352*, 575−580.
(23) Yu, Z.; Hecht, S. *Angew. Chem., Int. Ed.* **2011**, *50*, 1640−1643.
(24) Kay, E. R.; Leigh, D. A.; Zerbetto, F. *Angew. Chem., Int. Ed.* **2007**, *46*, 72−191.
(25) Moretto, A.; Menegazzo, I.; Crisma, M.; Shotton, E. J.; Nowell, H.; Mammi, S.; Toniolo, C. *Angew. Chem., Int. Ed.* **2009**, *48*, 8986−8989.
(26) Byrne, L.; Solà, J.; Boddaert, T.; Marcelli, T.; Adams, R. W.; Morris, G. A.; Clayden, J. *Angew. Chem., Int. Ed.* **2014**, *53*, 151−155.
(27) Le Bailly, B. A. F.; Byrne, L.; Diemer, V.; Foroozandeh, M.; Morris, G. A.; Clayden, J. *Chem. Sci.* **2015**, *6*, 2313−2322.
(28) Brown, R. A.; Diemer, V.; Webb, S. J.; Clayden, J. *Nat. Chem.* **2013**, *5*, 853−860.
(29) Pengo, B.; Formaggio, F.; Crisma, M.; Toniolo, C.; Bonora, G. M.; Broxterman, Q. B.; Kamphius, J.; Saviano, M.; Iacovino, R.; Rossi, F.; Benedetti, E. *J. Chem. Soc., Perkin Trans. 2* **1998**, 1651−1658.
(30) Clayden, J.; Castellanos, A.; Solà, J.; Morris, G. A. *Angew. Chem., Int. Ed.* **2009**, *48*, 5962−5965.
(31) Solà, J.; Fletcher, S. P.; Castellanos, A.; Clayden, J. *Angew. Chem., Int. Ed.* **2010**, *49*, 6836−6839.
(32) Ousaka, N.; Takeyama, Y.; Iida, H.; Yashima, E. *Nat. Chem.* **2011**, *3*, 856−861.
(33) Ousaka, N.; Takeyama, Y.; Yashima, E. *Chem. - Eur. J.* **2013**, *19*, 4680−4685.
(34) Toniolo, C.; Crisma, M.; Formaggio, F.; Peggion, C. *Biopolymers* **2001**, *60*, 396−419.
(35) Venkatraman, J.; Shankaramma, S. C.; Balaram, P. *Chem. Rev.* **2001**, *101*, 3131−3152.
(36) Hummel, R.-P.; Toniolo, C.; Jung, G. *Angew. Chem., Int. Ed. Engl.* **1987**, *26*, 1150−1152.
(37) Solà, J.; Morris, G. A.; Clayden, J. *J. Am. Chem. Soc.* **2011**, *133*, 3712−3715.
(38) Toniolo, C.; Polese, A.; Formaggio, F.; Crisma, M.; Kamphuis, J. *J. Am. Chem. Soc.* **1996**, *118*, 2744−2745.
(39) Polese, A.; Formaggio, F.; Crisma, M.; Valle, G.; Toniolo, C.; Bonora, G. M.; Broxterman, Q. B.; Kamphuis, J. *Chem. - Eur. J.* **1996**, *2*, 1104−1111.
(40) De Poli, M.; De Zotti, M.; Raftery, J.; Aguilar, J. A.; Morris, G. A.; Clayden, J. *J. Org. Chem.* **2013**, *78*, 2248−2255.
(41) Crisma, M.; Toniolo, C. *Biopolymers* **2015**, *104*, 46−64.
(42) Brown, R. A.; Marcelli, T.; De Poli, M.; Solà, J.; Clayden, J. *Angew. Chem., Int. Ed.* **2012**, *51*, 1395−1399.
(43) De Poli, M.; Byrne, L.; Brown, R. A.; Solà, J.; Castellanos, A.; Boddaert, T.; Wechsel, R.; Beadle, J. D.; Clayden, J. *J. Org. Chem.* **2014**, *79*, 4659−4675.
(44) Wüthrich, K. *NMR of Proteins and Nucleic Acids*; Wiley: New York, 1986.
(45) Altoè, P.; Haraszkiewicz, N.; Gatti, F. G.; Wiering, P. G.; Frochot, C.; Brouwer, A. M.; Balkowski, G.; Shaw, D.; Woutersen, S.; Buma, W. J.; Zerbetto, F.; Orlandi, G.; Leigh, D. A.; Garavelli, M. *J. Am. Chem. Soc.* **2009**, *131*, 104−117.
(46) Gowda, B. T.; Foro, S.; Shakuntala, K.; Fuess, H. *Acta Crystallogr., Sect. E: Struct. Rep. Online* **2011**, *E67*, o117.
(47) Shakuntala, K.; Foro, S.; Gowda, B. T. *Acta Crystallogr., Sect. E: Struct. Rep. Online* **2011**, *E67*, o1415.
(48) Gatti, F. G.; León, S.; Wong, J. K. Y.; Bottari, G.; Altieri, A.; Farran Morales, M. A.; Teat, S. J.; Frochit, C.; Leigh, D. A.; Brouwer, A. M.; Zerbetto, F. *Proc. Natl. Acad. Sci. U. S. A.* **2003**, *100*, 10−14.
(49) Li, T.; Budt, K.-H.; Kishi, Y. *J. Chem. Soc., Chem. Commun.* **1987**, 1817−1819.
(50) Crisma, M.; Valle, G.; Formaggio, F.; Toniolo, C.; Bagno, A. *J. Am. Chem. Soc.* **1997**, *119*, 4136−4142.
(51) Crisma, M.; Moretto, A.; Formaggio, F.; Kaptein, B.; Broxterman, Q. B.; Toniolo, C. *Angew. Chem., Int. Ed.* **2004**, *43*, 6695−6699.
(52) Byrne, L.; Solà, J.; Clayden, J. *Chem. Commun.* **2015**, *51*, 10965−10968.
(53) Moretto, A.; Peggion, C.; Formaggio, F.; Crisma, M.; Kaptein, B.; Broxterman, Q. B.; Toniolo, C. *Chirality* **2005**, *17*, 481−487.
(54) Toniolo, C.; Bonora, G. M.; Barone, V.; Bavoso, A.; Benedetti, E.; Di Blasio, B.; Grimaldi, P.; Lelj, F.; Pavone, V.; Pedone, C. *Macromolecules* **1985**, *18*, 895−902.
(55) Nair, C. M. K.; Vijayan, M. *Acta Crystallogr., Sect. B: Struct. Crystallogr. Cryst. Chem.* **1980**, *B36*, 1498−1500.
(56) Toniolo, C.; Bonora, G. M.; Crisma, M.; Benedetti, E.; Bavoso, A.; Di Blasio, B.; Pavone, V.; Pedone, C. *Int. J. Pept. Protein Res.* **1983**, *22*, 603−610.
(57) Crisma, M.; Formaggio, F.; Toniolo, C. *Acta Crystallogr., Sect. C: Cryst. Struct. Commun.* **2000**, *C56*, 695−696.
(58) Crisma, M.; Valle, G.; Formaggio, F.; Toniolo, C.; Broxterman, Q. B.; Kamphuis, J. *Z. Kristallogr. - New Cryst. Struct.* **1998**, *213*, 315−316.
(59) Crisma, M.; Valle, G.; Moretto, V.; Formaggio, F.; Toniolo, C. *Pept. Res.* **1995**, *8*, 187−190.
(60) Crisma, M.; Formaggio, F.; Pantano, M.; Valle, G.; Bonora, G. M.; Toniolo, C.; Schoemaker, H. E.; Kamphuis, J. *J. Chem. Soc., Perkin Trans. 2* **1994**, 1735−1742.
(61) Valle, G.; Crisma, M.; Pantano, M.; Formaggio, F.; Toniolo, C.; Kamphuis, J. *Z. Kristallogr. - Cryst. Mater.* **1993**, *208*, 259−262.
(62) Desiraju, G. R.; Steiner, T. *The Weak Hydrogen Bond*; Oxford University Press: New York, 1999.
(63) Boddaert, T.; Solà, J.; Helliwell, M.; Clayden, J. *Chem. Commun.* **2012**, *48*, 3397−3399.
(64) Maury, J.; Le Bailly, B. A. F.; Raftery, J.; Clayden, J. *Chem. Commun.* **2015**, *51*, 11802−11805.
(65) Le Bailly, B. A. F.; Clayden, J. *Chem. Commun.* **2014**, *50*, 7949−7952.

DOI: 10.1021/jacs.6b04435
J. Am. Chem. Soc. 2016, 138, 8007−8018